Novel microchip for *in situ* TEM imaging of living organisms and bio-reactions in aqueous conditions†

Kuo-Liang Liu,[a] Chien-Chen Wu,[b] Ying-Jung Huang,[b] Hwei-Ling Peng,[b] Hwan-You Chang,[c] Pin Chang,[d] Long Hsu[e] and Tri-Rung Yew*[a]

Received 26th March 2008, Accepted 26th June 2008
First published as an Advance Article on the web 12th September 2008
DOI: 10.1039/b804986f

A novel and disposable microchip (K-kit) with SiO_2 nano-membranes was developed and used as a specimen kit for *in situ* imaging of living organisms in an aqueous condition using transmission electron microscopy (TEM) without equipment modification. This K-kit enabled the successful TEM observation of living *Escherichia coli* cells and the tellurite reduction process in *Klebsiella pneumoniae.* The *K. pneumoniae* and *Saccharomyces cerevisiae* can stay alive in K-kit after continuous TEM imaging for up to 14 s and 42 s, respectively. Besides, different tellurite reduction profiles in cells grown in aerobic and anaerobic environments can be clearly revealed. These results demonstrate that the K-kit developed in this paper can be useful for observing living organisms and monitoring biological processes *in situ*.

Introduction

Cellular ultrastructures[1–3] are most commonly examined using transmission electron microscopy (TEM). Although TEM can achieve atomic scale resolution, specimens for TEM observation must be either dry[4–6] or frozen[7–10] due to TEM's high-vacuum operation requirements. Dehydration often causes structural distortion of the sample, and many biological processes cannot be monitored in real time in TEM studies.

Previous studies have attempted to develop environmental TEM for observing wet samples.[11–15] Heide first introduced a specimen chamber (Elmiskop I) to replace conventional TEM sample holders for biological applications.[12] Parsons further modified the specimen chamber by controlling the pressure of various gas and water vapors around the specimen to successfully produce a TEM image of a living human leukocyte.[13] Similar approaches were also applied to observe liquid–solid polymerization reactions[14] and electrochemical metal deposition.[15–17] The similar concept has been successfully developed for imaging liquids, cells, and other wet samples in the scanning electron microscopy by Thiberge *et al.*[18,19] However, it is desirable to develop a disposable specimen kit that can fit in standard TEM sample holders without modification, making high resolution *in situ* imaging of living cells or samples in aqueous solution a powerful tool for many researchers.

To provide an alternative way for living cell imaging in TEM other than environmental TEM that has advantages of controlling various gas and water vapors of specimens, we developed a novel and disposable microchip that functions as a specimen kit, with the advantages of being able to fit into commercially-available TEM and avoiding the contamination of samples of the TEM holder or between samples. This microchip is equipped with SiO_2 nano-membranes that seal living organisms in aqueous condition and shield the subject from the TEM vacuum environment using microelectromechanical system (MEMS) techniques. Using prokaryotic cells such as *Escherichia coli* (*E. coli*) JM109 [pmrkABCD$_{v3}$F][20,21] and *Klebsiella pneumoniae* (*K. pneumoniae*) CG43S3,[22–25] and eukaryotic cells like yeast *Saccharomyces cerevisiae* (*S. cerevisiae*) AH109[26] as examples, we demonstrated in this study the feasibility of this microchip for living organism observation and biological process *in situ* monitoring.

The reasons that we use *K. pneumoniae*, *E. coli*, and *S. cerevisiae* as examples in this study are as follows. *K. pneumoniae* is a ubiquitous bacterium causing many infection in immunocompromised individuals who are hospitalized.[23,27] Heavy metals at specific concentrations form complex compounds to cause a toxic effect in the bacteria, although many genes of bacteria will be involved in maintaining homeostasis of the heavy-metal ion. For example, tellurium compounds have been used as antimicrobial and therapeutic agents.[28] However, an *E. coli* terZABCDE homolog was observed in the large virulence plasmid pLVPK of *K. pneumoniae* CG43S3 and was responsible for tellurite resistance.[23,29,30] *S. cerevisiae*[26] or baker's yeast is the simplest eukaryote and an important model organism.

[a]*Department of Materials Science and Engineering, National Tsing-Hua University, 101, Sec.2, Kuang-Fu Road, Hsinchu, Taiwan 300. E-mail: tryew@mx.nthu.edu.tw; Fax: 886-3-5722366; Tel: 886-936347230*
[b]*Department of Biological Science and Technology, National Chiao-Tung University, 1001, Ta-Hsueh Road, Hsinchu, Taiwan 300*
[c]*Institute of NanoEngineering and MicroSystems, National Tsing-Hua University, 101, Sec.2, Kuang-Fu Road, Hsinchu, Taiwan 300*
[d]*Microsystems Technology Center, ITRI South, Industrial Technology Research Institute, Tainan, Taiwan 709*
[e]*Department of Electrophysics, National Chiao-Tung University, 1001, Ta-Hsueh Road, Hsinchu, Taiwan 300*

† Electronic supplementary information (ESI) available: Fig. S1, fluorescence images of four *K. pneumoniae* samples for pre-TEM, and post-continuous TEM; Fig. S2, fluorescence images of the *K. pneumoniae* pre- and post-accumulated TEM for different durations. See DOI: 10.1039/b804986f

Experimental

Microchip fabrication

The microchip consists of two substrates with two aligned SiO_2 nano-membranes as an observation window that can be penetrated by an electron beam. We used SiO_2 membranes as thin as possible in order to decrease electron scattering by SiO_2 membranes. However, the thickness of SiO_2 membrane is limited by the Si to SiO_2 etching selectivity (about 520 ± 78), SiO_2 etching rate (about 0.9 ± 0.1 nm min^{-1} at 65 °C) tetraethylammonium hydroxide (TMAH; 20% in H_2O)[31,32] etchant, and especially Si_3N_4 to SiO_2 selectivity (30 ± 4.5) phosphoric acid (H_2PO_3; 65% in H_2O) etchant at 90 °C.

Based on above design and process optimization, the fabrication of 9 nm of SiO_2 membrane is feasible *via* wet-etching process. First, each substrate is composed of a double-side-polished silicon with 9 nm-thick SiO_2 membranes formed by thermal oxidation from O_2 at 900 °C. Following that, 1500 nm-thick Si_3N_4 films were deposited as mask layers on the SiO_2 membranes (Fig. 1a) by low pressure chemical vapor deposition from SiH_2Cl_2/NH_3 at 850 °C. On one side of the substrate, Si_3N_4 layer and SiO_2 membranes were coated with photoresist (PR) and patterned to form a 850 μm 850 μm square by photolithography (Fig. 1b) and reactive ion etching (RIE) processes to expose a portion of silicon (Fig. 1c), followed by PR stripping (Fig. 1d). Subsequently, the exposed silicon was etched with a TMAH solution at 65 °C. Residual Si_3N_4 film was then removed by hot H_2PO_3 solution at 90 °C for about 3 min to form a (150 ± 10) μm × (150 ± 10) μm observation window composed of 9 nm-thick SiO_2 (Fig. 1e). Two substrates were then stacked face-to-face by aligning their observation windows and bonded together by epoxy resins with high viscosity (10000 cps/25 °C), which was applied carefully onto the corners of the substrate to prevent it from contaminating the viewing window (Fig. 1f).

This special microchip is named as K-kit for its cross-section view looks like two "K"s stacked together back-to-back, as shown in Fig. 1f. The substrates were originally diced to form pieces 2.8 mm × 2.8 mm before the wet etching by TMAH, while the substrates shrank to about 1.3 mm × 1.3 mm (*i.e.*, a diagonal dimension of about 1.8 mm) after etching. The K-kit was then applied with appropriate amount of epoxy resins on the corners carefully and adhered onto copper grid which was previously cut in the center to form a hole with a diameter of about 1.8 mm. The K-kit adhered to copper grid then could be loaded onto the commonly-used TEM sample holder.

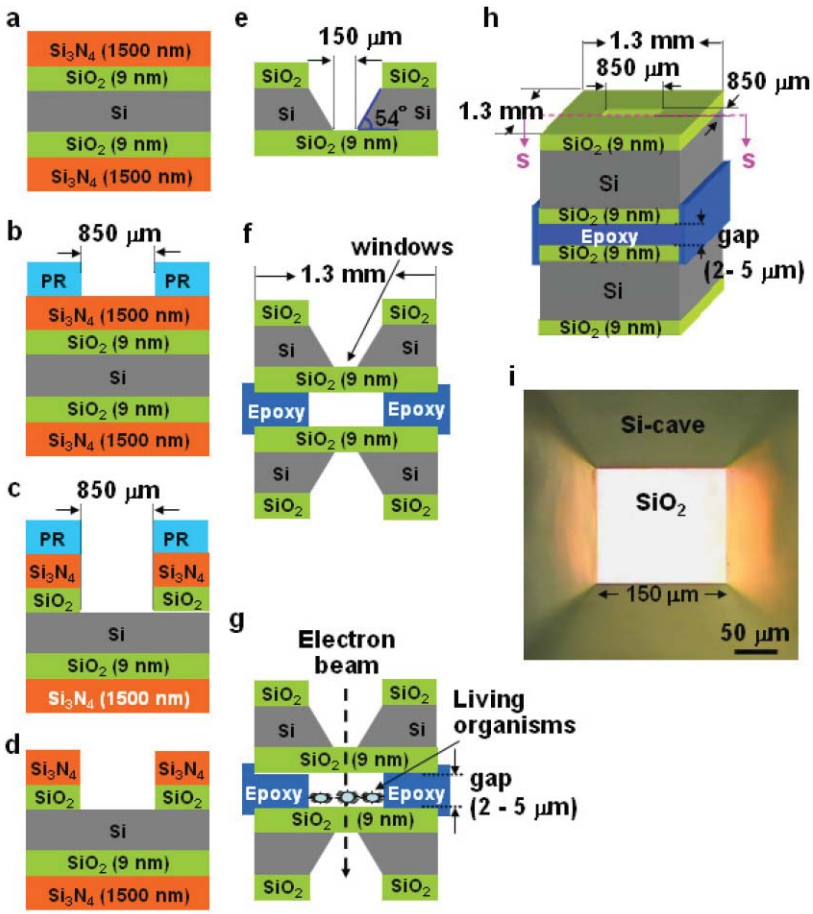

Fig. 1 Cross-section schematics of the process flow for fabricating a K-kit, (a) SiO_2 membrane and Si_3N_4 layer deposition on Si, (b) PR coating and patterning, (c) SiO_2 and Si_3N_4 etching by RIE, (d) PR stripping, (e) Si etching and Si_3N_4 stripping, (f) two substrates stacked face-to-face, (g) living organisms filling the specimen, (h) a final 3D schematic of the K-kit, with the cross-section view along s–s depicted in (g), and (i) the OM image of the top view of a K-kit with Si-cave and SiO_2 nano-membrane (observation window). There are 115 K-kits fabricated in total ($n = 115$).

This journal is © The Royal Society of Chemistry 2008

The epoxy resins composed of epoxy and polyamine agents applied with 1 μm polystyrene beads (Polysciences Inc.). The volume of epoxy resins normally expanded after polymerization, which could result in the formation of a 2–5 μm gap between the two substrates. The 2–5 μm gap was fabricated considering the size of *E. coli* and *K. pneumoniae* cells, which were about 0.5–1 μm in height. The increase of gap height may degrade the TEM resolution because of increased electron scattering. The curing time of epoxy resin is about 10 min for its polymerization at room temperature. Epoxy resin was also applied to the edge of both substrates after the gap was filled with the bacterial suspension (Fig. 1g).

Compared to the attempts made by Thiberge *et al.*[18,19] using an apparatus for imaging liquids, cells, and other wet samples in SEM, the similarities between Thiberge's work and this work are that both used thin membrane to enclose and protect the aqueous samples from the vacuum environment. Besides, the polyimide membranes used by Thiberge *et al.* and the silicon oxide (SiO_2) membranes used in this work were all thin enough for energetic electrons to pass through for imaging.

However, there are differences between the work reported by Thiberge *et al.* and this work. Thiberge *et al.* used an organic polyimide membrane of 145 nm in thickness on top as a viewing window, o-rings as a sealing material to against external pressure, and two stainless steel pieces as substrates in their apparatus for SEM imaging, whereas we used two inorganic 9 nm-thick SiO_2 membranes with one on top and the other at bottom as the viewing window, epoxy resin as a sealing material, and Si substrates in our K-kit for TEM imaging.

Preparation of bacteria stained with fluorescent dye and negative dye

Both *E. coli* JM109 [pmrkABCD$_{v3}$F][20,21] cells supplemented with Ampicillin (100 μg ml^{-1}) and *K. pneumoniae* CG43S3[22–25] cells were grown in Luria-Bertani (LB) broth at 37 °C till mid-exponential phase. *S. cerevisiae* AH109[26] were grown in YPD medium (1% yeast extract, 2% peptone, 2% glucose) at 30 °C for 48 h. The cells' viability was determined by staining with the LIVE/DEAD® Baclight™ Bacterial Viability Kit (Invitrogen Carlsbad)[33–35] for 15 min. The living bacteria fluoresce green, whereas dead bacteria fluoresce red. Besides, the bacteria may fluoresce yellow or orange when green and red fluorescent dyes both exist in bacteria. The yellow or orange bacteria were considered as dead cells as the red-fluorescent propidium iodide only enters dead bacteria with damaged cell membranes.

Negative staining for TEM imaging was achieved by incubating with sodium phosphotungstate (PTA; 2% w/v in DI water) for 5 s. Based on our own measurement, the minimum inhibitory concentration of PTA to *E. coli* was approximately 12 mg ml^{-1}. No detectable toxicity to *E. coli* cells was noted at 2% w/v PTA (~ 0.02 mg ml^{-1}).

Transmission electron microscopy (TEM) and fluorescence microscopy

The TEM imaging in this work was conducted using a JEOL JEM-2010 (200 KeV, Lab_6). Each image was captured with a minimum exposure operation[36] (current density = 30 pA cm^{-2} or 1.8×10^{-6} electrons nm^{-2} s^{-1}, exposure time = 2.8 s). Tellurium was characterized by field emission TEM (JEM-2100 F, 200 KeV) equipped with an ISIS 300 energy dispersive X-ray spectrometer (EDS). The examination of living or dead cells was carried out using an epi-fluorescence microscope (BX51, Olympus).

Results and discussion

TEM specimen kit (K-kit) design and fabrication

Fig. 1a–g show the fabrication process using MEMS techniques for the 1.3 mm × 1.3 mm K-kit with a (150 ± 10) μm × (150 ± 10) μm electron-transparent SiO_2 nano-membrane as an observation window. This K-kit was designed and developed to fit commonly-used TEM without equipment modification. Bacterial suspension was allowed to fill the space between the two SiO_2 nano-membranes and sealed with epoxy resins (Fig. 1h). The space height is about 2–5 μm, controlled by using 1 μm polystyrene beads (mixed in the epoxy resins) as a spacer. The image in Fig. 1i was taken by optical microscope, and showed a top view of the K-kit with a Si-cave and SiO_2 nano-membrane (observation window).

Viability of bacterial cells sealed in the K-kit

The first step in this study was to examine the survival ratio of bacterial cells sealed in the K-kit. *K. pneumoniae* CG43S3 cells in mid-log phase were stained with the LIVE/DEAD® Baclight™ Bacterial Viability Kit, immersed in LB, and sealed in the K-kit (Fig. 2a–c) for different time periods. The results for sealed cells were compared with those of unsealed cells (Fig. 2d–f). The bacterial survival ratio in the sealed K-kit was about 95%

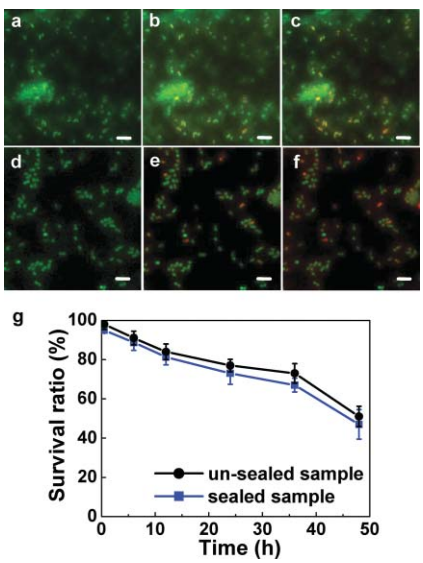

Fig. 2 Viability of *K. pneumoniae* CG43S3 cells in K-kits. The bacteria were stained with the LIVE/DEAD® Baclight™ bacterial viability kit and then loaded into the K-kit. Fluorescence images of *K. pneumoniae* in the sealed (a)–(c) and unsealed (d)–(f) K-kits, were taken sequentially at 30 min, 24 h and 48 h, respectively. The bacterial survival *versus* time ratios for both sealed and unsealed samples are plotted (g). The mean numbers of cells in sealed and unsealed conditions are 127 and 112, respectively. Experiments were repeated for five different samples for each data point ($n = 5$).

after 30 min and gradually decreased to 47% at 48 h, whereas the values of unsealed samples were 99% and 51%, respectively (Fig. 2g). Experiments were repeated for five different samples at each data point ($n = 5$). Most of the subsequent studies were performed within 12 h after sealing to ensure that bacteria viability exceeded 80% before TEM imaging.

Viability of bacterial cells after TEM imaging

The viability of bacterial cells after TEM imaging was tested to check the limitation of using K-kit for the living cell observation in TEM. *E. coli* JM109 cells were pre-stained with the LIVE/DEAD® Kit, then negatively stained with PTA and sealed in K-kits. Prior to TEM exposure, most of the *E. coli* cells showed green fluorescence, indicating that they were still alive (Fig. 3a). After TEM imaging with minimum exposure operation (current density = 30 pA cm^{-2}, exposure time = 2.8 s) at 200 KeV electron beam (Fig. 3b), the *E. coli* cells remained viable and continued to emit green fluorescence (Fig. 3c). Similar results were obtained from ten different TEM samples ($n = 10$).

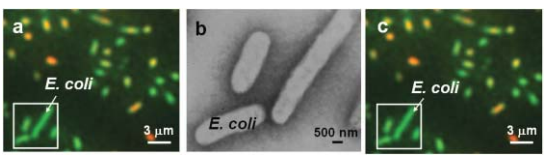

Fig. 3 Viability of *E. coli* JM109 cells in K-kits. (a) Fluorescent images before TEM exposure, (b) TEM image taken from the boxed area indicated in (a) at 200 KeV for 2.8 s, and (c) fluorescent images after TEM exposure. Experiments were repeated for ten different samples ($n = 10$).

Similar experiments were applied to *K. pneumoniae* CG43S3, which was also used for subsequent tellurite reduction experiments, and yeast *S. cerevisiae* AH109. The fluorescence image (Fig. 4a–4d) reveals that *K. pneumoniae* CG43S3 and *S. cerevisiae* cells were all alive before electron beam exposure. Several cells at different locations ($\geqq 10$ μm apart, much greater than the 3 μm diameter of the electron beam) in the same kit were then exposed to a 200 KeV electron beam for various durations at a low current density (~30 pA cm^{-2}). Most of the treated *K. pneumoniae* and *S. cerevisiae* cells could stay alive after the continuous electron beam exposure for up to 14 s and 42 s, respectively (Fig. 4e). The same *K. pneumoniae* results as above were obtained for four different TEM samples ($n = 4$) (see the ESI: Fig. S1).

Besides, the fluorescence images of *K. pneumoniae* cells under accumulated electron beam exposure revealed that bacteria could stay alive up to 19.6 s. The interval between each electron beam exposure (2.8 s) was 10 min (see the ESI: Fig. S2).

In situ TEM observation of tellurite reduction by *K. pneumoniae*

Characterization of tellurite-nanopartical reduction in *K. pneumoniae* using TEM. The K-kit was then used to monitor tellurite reduction by *K. pnuemoniae in situ*. *K. pnuemoniae* CG43S3 cells were immersed in LB containing K_2TeO_3 (40 μg ml^{-1}) in deionized water for 4 h, and then loaded into the specimen kit. This sample was dried for TEM imaging (Fig. 5a). Energy dispersive X-ray spectrometer (EDS) mapping in boxed area

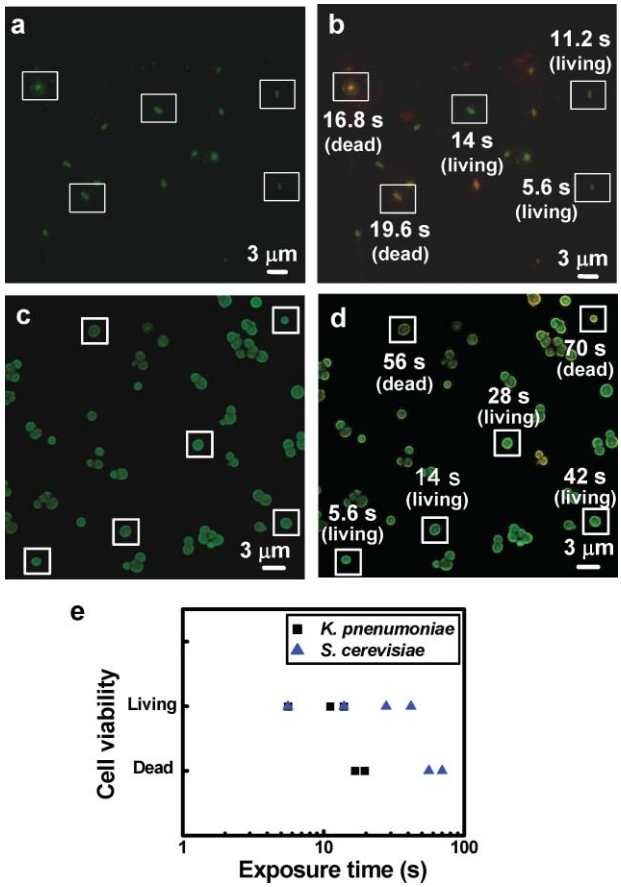

Fig. 4 Fluorescence images of the *K. pneumoniae* CG43S3 (a) pre- and (b) post-continuous TEM (200 KeV) electron beam exposure for different durations, and those of *S. cerevisiae* in (c) and (d), respectively. (e) The plot shows the viability of *K. pneumoniae* CG43S3 (square) and *S. cerevisiae* cells (triangle) *versus* electron beam exposure time.

A in Fig. 5a indicates the presence of tellurium (Te) in *K. pneumoniae* cells (Fig. 5b). A dark-field TEM image (Fig. 5c)

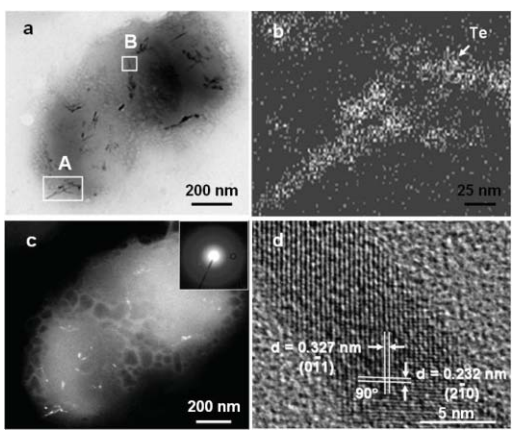

Fig. 5 Verification of the presence of Te in *K. pneumoniae* CG43S3. (a) TEM images of a *K. pnuemoniae* cell incubated in a K_2TeO_3 solution for 4 h, (b) EDS mapping of tellurium in boxed area A as indicated in (a), (c) dark-field image diffracted from Te {301} planes (d{301} = 1.25 Å), (d) lattice-image of microcrystalline Te nanoparticles, taken from the boxed area B as indicated in (a). Each analysis was repeated with three different samples ($n = 3$).

This journal is © The Royal Society of Chemistry 2008

also shows that Te grains of 18 nm in diameter formed on the {301} plane based on the 0.125 nm lattice-spacing according to Joint Committee on Powder Diffraction Standards (JCPDS) card number 36–1452 and the calculation from diffraction ring (inset, Fig. 5c) by the Bragg equation, $d = \lambda L/R$. Here, d, λ, L and R represent lattice-spacing, electron beam wavelength, TEM camera length and ring radius on the photographic film, respectively. The microcrystalline Te nanoparticles appearing in the boxed area-B in Fig. 5a were further identified by the high-resolution TEM lattice-image (Fig. 5d).[37] This two-dimensional lattice image represents the array of Te atoms in tellurium crystal formed by the *K. pneumoniae* cells.

***In situ* imaging of tellurite reduction in *K. pneumoniae* by TEM.** This study also conducted *in situ* monitoring of the tellurite reduction using the same living *K. pneumoniae* CG43S3 cells. TEM images were taken sequentially on the same cell at minimum exposure operation[36] (current density = 30 pA cm^{-2}, exposure time = 2.8 s) after the cell was sealed in the kit for 45 min (Fig. 6a), 50 min (Fig. 6b), 2.5 h (Fig. 6c), and 12.5 h (Fig. 6d), with the accumulated time of electron beam exposure less than 19.6 s to ensure the *K. pneumoniae* CG43S3 cells remained alive. Bubble-like vesicles occasionally appeared in sealed samples during TEM imaging, and were hard to remove as the kits were sealed against vacuum. This phenomenon was also observed previously in wet sample observation using environmental TEM.[13] For comparison, *K. pneumoniae* cells grown aerobically in the glass tube containing Luria-Bertani mixed K_2TeO_3 (40 μg ml^{-1}) were used as controlled samples. They were applied on Formvar/carbon copper grids for TEM imaging after they had grown for 45 min, 50 min, 2.5 h, and 12.5 h, respectively, with the results shown in Fig. 6e–h, respectively. The quantifications of Te-particle density and Te-particle size *versus* incubation time of *K. pneumoniae* in K_2TeO_3 are given in Fig. 6i and j, respectively, according to the TEM images (Fig. 6a–h).

It can be observed that the density of Te nanoparticles formed by *K. pneumoniae* within the K-kit (sealed samples) was lower than that in the controlled samples (Fig. 6i), while the particle size was larger for the same incubation duration (Figs. 6j). The density of Te nanoparticles for both sealed and controlled samples initially increased with time for 50 min then decreased, possibly due to particle fusion. The Te-particle size initially increased with mixing time and then saturated after 50 min for controlled samples, while kept increasing for sealed samples. At 12.5 h the grain size grew to 160 nm for the sealed samples.

The different morphologies of Te nanoparticles between sealed and controlled samples might be due to the lower tellurite reduction activity of *K. pneumoniae* in an anaerobic environment. This in turn led to the formation of more localized and fewer Te nanoparticles than those of the *K. pneumoniae* grown in aerobic environments. These similar results were obtained for three different samples ($n = 3$). However, the mechanisms causing this distinction are worthy of further investigation.

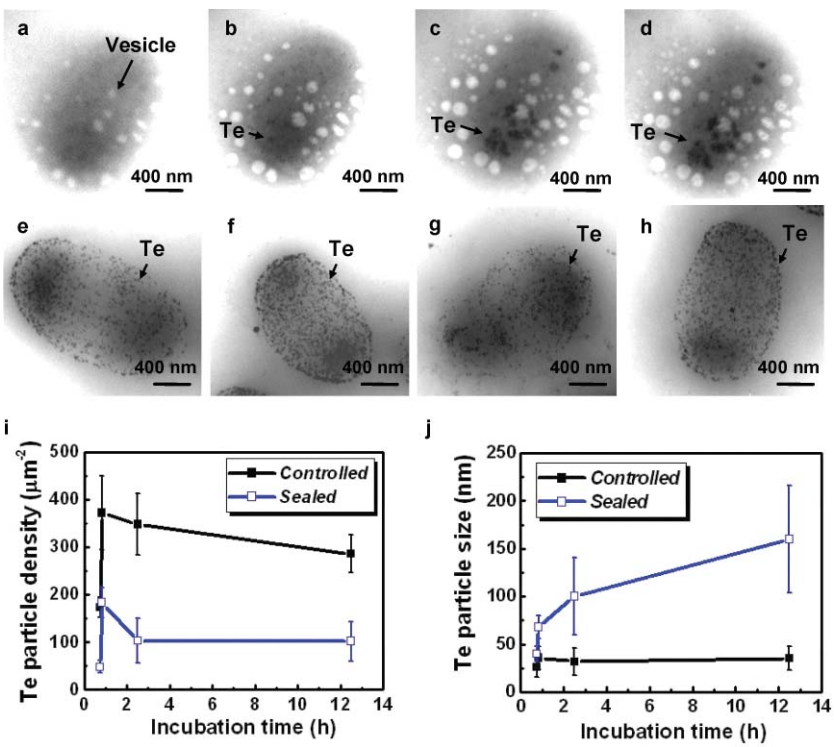

Fig. 6 *In situ* monitoring of tellurite reduction in *K. pneumoniae* CG43S3. The bacterial cells were incubated in LB containing K_2TeO_3. TEM images of the same *K. pneumoniae* cell after tellurite reduction for (a) 45 min, (b) 50 min, (c) 2.5 h, and (d) 12.5 h in the sealed K-kit. Vesicles (assumed to be gas bubbles) appeared during TEM imaging. TEM images of *K. pneumoniae* cells grown aerobically in the glass tube containing Luria-Bertani mixed K_2TeO_3 (40 μg ml^{-1}) as controlled samples, which were applied on Formvar/carbon copper grids for TEM imaging after their tellurite reduction for (e) 45 min, (f) 50 min, (g) 2.5 h, and (h) 12.5 h, respectively. Each image was exposed under a TEM electron beam for 2.8 s. Similar results were obtained for from three different samples for (a–d), $n = 3$, and four different samples for (e–h), $n = 4$. The plots of (i) Te-particle density and (j) Te-particle size *versus* incubation time of *K. pneumoniae* in K_2TeO_3 solution according to TEM images (Fig. 6a–h).

The comparisons between above TEM observation with previous works are discussed as following. In 1962, Heide[12] first imaged the water droplets of 0.5 μm in diameter using 400 nm SiO-film as a viewing window in TEM. Then Parsons[13] utilized carbon-Formvar film as viewing window to obtain a TEM image of 0.3 μm × 1 μm *Coliform* bacteria immersed in water in 1974. In 2003, Williamson[15] observed 5 nm Cu grains in electrolyte with *in situ* TEM. However, we can observe the living 0.5 μm × 1 μm *K. pnenumoniae* cells and 1 μm × 2 μm *E. coli* cells immersed in the solution (LB). Besides, the minimum 40 nm Te particles in *K. pnenumoniae* cells were also observed in this work, where the relatively lower resolution was mostly due to the fact that Te was in the bacterial cells which increased the electron scattering

Conclusions

This paper describes the development of a disposable and simple to use microchip that functions as a SiO_2 nano-membrane specimen kit (K-kit) for TEM imaging of living cells *in situ* in aqueous condition. The 1.3 mm × 1.3 mm K-kit fits perfectly on most TEM models without equipment modification. The TEM imaging of living cells was achieved with the use of the K-kit, and the *K. pneumoniae* and yeast *S. cerevisiae* cells could stay alive after being continuously exposed to a 200 KeV electron beam for up to 14 s and 42 s, respectively, at a low current density (~30 pA cm^{-2} or 1.8×10^{-6} electrons nm^{-2} s^{-1}). Most importantly, the kit allows *in situ* monitoring of a biological process, namely tellurite reduction in *K. pneumoniae*, by TEM. Different tellurite reduction profiles in cells grown in aerobic and anaerobic environments were observed. The minimum 40 nm Te particles formed in *K. pneumoniae* can be observed using the K-kit. The electron scattering by the micro-scale cells is more significant than 9 nm-thick SiO_2 in this work, so that the resolution is limited by the size of the cells. The thinnest feasible thickness of SiO_2 membrane is determined by the Si to SiO_2 etching selectivity, SiO_2 etching rate, and especially the Si_3N_4 to SiO_2 selectivity of the wet-etching process. Although the increase of SiO_2 thickness may enhance the strength of the SiO_2 membrane to allow larger viewing window, it may also degrade the resolution on TEM imaging of *E. coli* due to more electron scattering by SiO_2.

To improve the viability of cells, it is suggested to grow bacteria directly on the SiO_2 membrane in suspension to reduce other preparation process unfavorable to cells before TEM imaging. If a more sensitive charge coupled device (CCD) is used to capture TEM images under lower current and shorter exposure time, or more space can be created inside the K-kit to maintain abundant nutrition, the viability of cells can be improved. The development of quantitatively controlling the liquid content in the K-kit is required to reduce the electron scattering and then improve the resolution. However, the K-kit exhibits potentially useful application for the study of magnetic material not allowed to be directly exposed to electron beam in TEM, and the *in situ* monitoring and observation of biological, chemical, and physical reaction in aqueous condition.

Acknowledgements

This work was supported by National Science Council under project numbers NSC 94–2120-M009–015 and NSC 95–2120-M009–005. The authors appreciate the support for the furnace for SiO_2 and Si_3N_4 deposition and TEM from NCTU-NFC, the precision translation stage from Y. J. Su at NCTU, the RIE and photolithography from Prof. C. N. Liao at NTHU, and the wafer bonding from NTHU-CMMM.

References

1 G. Leid, C. A. Speer and M. A. Jutila, *J. Leuk. Biol.*, 1998, **64**, 104–107.
2 L. T. Salgado, N. B. Viana, L. R. Andrade, R. N. Leal, B. A. P. da Gama, M. Attias, R. C. Pereira and G. M. Amado Filho, *J. Struct. Biol.*, 2008, **162**, 345–355.
3 A. E. Yakushevska, M. N. Lebbink, W. J. C. Geerts, L. Spek, E. G. van Donselaar, K. A. Jansen, B. M. Humbel, J. A. Post, A. J. Verkleij and A. J. Koster, *J. Struct. Biol.*, 2007, **159**, 81–391.
4 E. Hahn, P. Wild, U. Hermanns, P. Sebbel, R. Glockshuber, M. Häner, N. Taschner, P. Burkhard, U. Aebi and S. A. Müller, *J. Mol. Biol.*, 2002, **323**, 845–857.
5 G. Reguera, K. D. McCarthy, T. Mehta, J. S. Nicoll, M. T. Tuominen and D. R. Lovley, *Nature*, 2005, **435**, 1098–1101.
6 P. Goldberg-Oppenheimer and O. Regev, *Small*, 2007, **3**, 1894–1899.
7 D. R. Beniac, D. D. Wood, N. Palaniyar, F. P. Ottensmeyer, M. A. Moscarello and G. Harauz, *J. Stuct. Biol.*, 2000, **129**, 80–95.
8 A. Al-Amoudi, J. J. Chang, A. Leforestier, A. McDowall, L. M. Salamin, L. P. Norlén, K. Richter, N. S. Blanc, D. Studer and J. Dubochet, *EMBO J.*, 2004, **23**, 3583–3588.
9 N. Matsko and M. Mueller, *J. Struct. Biol.*, 2005, **152**, 92–103.
10 O. Medalia, I. Weber, A. S. Frangakis, D. Nicastro, G. Gerisch and W. Baumeister, *Science*, 2007, **298**, 1209–1213.
11 P. L. Hansen, J. B. Wagner, S. Helveg, J. R. Rostrup-Nielsen, B. S. Clausen and H. Topsøe, *Science*, 2002, **295**, 2053–2055.
12 H. G. Heide, *J. Cell Biol.*, 1962, **13**, 147–152.
13 D. F. Parsons, *Science*, 1974, **186**, 407–414.
14 P. L. Gai, *Top. Catal.*, 2002, **21**, 161–173.
15 M. J. Williamson, R. M. Tromp, P. M. Vereecken, R. Hull and F. M. Ross, *Nat. Mater.*, 2003, **2**, 532–536.
16 A. Radisic, P. M. Vereecken, J. B. Hannon, P. C. Searson and F. M. Ross, *Nano Lett.*, 2006, **6**, 238–242.
17 A. Radisic, P. M. Vereecken, P. C. Searson and F. M. Ross, *Surf. Sci.*, 2006, **600**, 1817–1826.
18 S. Thiberge, A Nechushtan, D. Sprinzak, O. Gileadi, V. Behar, O. Zik, Y. Chowers, S. Michaeli, J. Schlessinger and Elisha Moses, *Proc. Natl. Acad. Sci. U. S. A.*, 2004, **101**, 3346–3351.
19 S. Thiberge, O. Zik and E. Moses, *Rev. Sci. Instrum.*, 2004, **75**, 2280–2289.
20 B. J. Chang, Y. J. Huang, C. H. Chan, H. Long, H. L. Peng, H. Y. Chang, T. R. Yew, C. H. Liu and S. Chi, *Biochem. Biophys. Res. Commun.*, 2006, **350**, 33–38.
21 Y. J. Huang, C. C. Wu, M. C. Chen, C. P. Fung and H. L. Peng, *Biochem. Biophys. Res. Commun.*, 2006, **350**, 537–542.
22 Y. C. Lai, H. L. Peng and H. Y. Chang, *J. Bacteriol.*, 2003, **185**, 788–800.
23 Y. T. Chen, H. Y. Chang, Y. C. Lai, C. C. Pan, S. F. Tsai and H. L. Peng, *Gene*, 2004, **337**, 189–198.
24 S. Vavrova, D. Valkova, H. Drahovska, J. Kokavec, J. Mravec and J. Turna, *BioMetals*, 2006, **19**, 453–460.
25 R. Podschun and U. Ullmann, *Clin. Microbiol. Rev.*, 1998, **11**, 589–603.
26 M. Surjit, B. Liu, P. Kumar, V. T. K. Chow and S. K. Lala, *Biochem. Biophys. Res. Commun.*, 2004, **317**, 1030–1036.
27 D. R. Schaberg, D. H. Culver and R. P. Gaynes, *Am. J. Med.*, 1991, **91**, 72S–75S.
28 P. M. Zadik, P. A. Chapman and C. A. Siddons, *J. Med. Microbiol.*, 1993, **39**, 155–158.
29 S. K. Chiang, Y. C. Lou and C. Chen, *Protein Sci.*, 2008, **17**, 785–789.
30 D. C. Old, *J. Gen. Microbiol.*, 1972, **71**, 149–157.
31 D. Resnik, D. Vrtacnik, U. Aljancic and S. Amon, *J. Micromech. Microeng.*, 2003, **13**, 26–34.
32 P. G. Miney and V. J. Cunnane, *Electrochim. Acta*, 2004, **49**, 1009–1018.
33 Molecular Probes, Inc., *LIVE/DEAD® BacLight™ Bacterial Viability Kits, Product Information Sheet*, Molecular Probes Inc., Eugene,

 This journal is © The Royal Society of Chemistry 2008

OR, 1997. The kit contains two nucleic acid stains such as green-fluorescent SYTO®9 dye which freely permeates living bacteria with intact cell membranes and red-fluorescent propidium iodide, which only enters dead bacteria with damaged cell membranes to displace green-fluorescent SYTO®9 dye. Living bacteria fluoresce green, whereas dead bacteria fluoresce red.
34 J. L. Alonso, S. Mascellaro, Y. Moreno, M. A. Ferrús and J. Hernández, *Appl. Environ. Microbiol.*, 2002, **68**, 5151–5154.
35 N. V. Quéric, T. Soltwedel and W. E. Arntz, *J. Microbiol. Methods*, 2004, **57**, 351–367.
36 JEOL Ltd, *JEM-2010 instruction manual, 5–57–60*, JEOL Ltd, Akishima, Tokyo, Japan, 1991. Minimum exposure operation reduces considerably the irradiation of electron beam on the bacteria. A small amount of electron beam is utilized to search the field to be photographed at low magnification. After determining the field, the position of desirable bacterium is saved. Following that, the magnification, focus, and brightness are adjusted on the nearby field. Finally, images are taken of the targeted bacterium automatically.
37 C. Adenis, V. Langer and O. Lindqvist, *Acta Crystallogr., Sect. C*, 1989, **45C**, 941–942.